EFFECTS OF ISOTHERMAL CRYSTALLIZATION ON THE MECHANICAL PROPERTIES OF A ELASTOMERIC MEDIUM CHAIN LENGTH POLYHYDROXYALKANOATE

A. Larrañaga[1,*], F. Pompanon[1], N. Gruffat[1], T. Palomares[2], A. Alonso-Varona[2], A. Larrañaga Varga[3], M.A. Fernandez-Yague[4,5], M.J.P. Biggs[4,5], J.R. Sarasua[1]

[1]Department of Mining-Metallurgy Engineering and Materials Science & POLYMAT, School of Engineering, University of the Basque Country (UPV/EHU) 480130 Bilbao, Spain

[2]University of the Basque Country (UPV/EHU), Faculty of Medicine and Odontology, Bilbao, Spain.

[3]SGIker, General Research Services, University of the Basque Country (UPV/EHU), B. Sarriena S/N, 48940 Leioa, Spain.

[4]CÚRAM - Centre for Research in Medical Devices, NUI Galway

[5]Department of Biomedical Engineering, NUI Galway

[*]Corresponding author: Email: aitor.larranagae@ehu.eus

Fax: +34 94 601 3930

Tel: + 34 946 017 138

Abstract

In the present study, the relationship between molecular structure and mechanical properties for a medium chain length polyhydroxyalkanoate (mcl-PHA) composed of 3-hydroxyoctanoate and 3-hydroxyhexanoate was elucidated. The mcl-PHA was crystallized from the melt at four different temperatures between its glass transition and melting point (37, 21, 3 and -21 ºC) and its molecular structure was analysed by means of differential scanning calorimetry (DSC) and wide-angle X-ray diffractometry (WAXD). The mechanical properties, which were analysed via tensile-tests and dynamic mechanical analysis (DMA), were clearly affected by the selected crystallization temperature and corresponding molecular structure of the polymer. In this sense, samples crystallized at 37, 21 and 3 ºC displayed higher secant moduli calculated at 2% ($E_{2\%}$~20 MPa) than the sample crystallized at -21 ºC ($E_{2\%}$~7 MPa) due to their higher crystallinity. Even if samples crystallized at 37, 21 and 3 ºC had very similar degree of crystallinity, their secant moduli calculated at 50, 100 and 200% ($E_{50\%}$, $E_{100\%}$ and $E_{200\%}$) and yield strength (σ_y) were clearly affected by the selected crystallization temperature, showing a positive correlation (i.e., higher crystallization temperatures and corresponding more ordered crystalline domains with narrower crystal distributions resulted in higher $E_{50\%}$, $E_{100\%}$ and $E_{200\%}$ values).

Keyword: polyhydroxyalkanoates, structure-property relations, mechanical properties, crystallization.

1. Introduction

Polyhydroxyalkanoates (PHAs) are a group of biodegradable and biocompatible thermoplastic polyesters which are synthesized by numerous microorganisms as intracellular carbon and energy storage compounds [1-4]. Unlike other conventional biodegradable synthetic thermoplastic polymers, in which great efforts are being made to either diminish the amount of residual catalyst in the final polymer [5-7] or to employ alternative catalysts with less toxicity [8, 9], there are no catalyst residues in PHAs thanks to a completely biosynthetic process. Additionally, PHAs with a wide range of physico-chemical, thermal and mechanical properties can be prepared via further physicochemical strategies such as copolymerization [10], blending [11], fabrication of composites [12, 13] or by tuning the biosynthesis conditions and monomeric units present [14]. For all the aforementioned reasons, PHAs have attracted increasing interest as biomaterials in various biomedical applications (e.g., vascular grafts [15], heart valves [16], nerve regeneration conduits [17], neuroelectrodes [18], as scaffold for hard- and soft-tissue engineering [19, 20], or as drug delivery vehicles [21]).

Among the PHA biomaterials in study, medium chain length PHAs (mcl-PHAs) (i.e., those that have between 6 and 14 carbon atoms in their structure) are of particular interest for those biomedical applications demanding elastomeric materials with soft mechanical properties thanks to their low crystallinity, low glass transition temperature and associated low tensile strength and high elongation at break [22]. In our previous work [23], a mcl-PHA copolymer composed of 94% and 6% of 3-hydroxyoctanoate and 3-hydroxyhexanoate [P(3HO-co-3HH)], respectively, was thoroughly characterized in terms of physico-chemical, thermal and mechanical properties. The studied material exhibited a glass transition temperature (T_g) of ~-35 ºC and a melting point (T_m) in the range between 48 and 62 ºC. Because of the low T_g and the low crystallization kinetics,

the polymer chains in the amorphous phase underwent supramolecular rearrangements which resulted in the development of crystalline domains. As a consequence, the strength related mechanical properties increased when the polymer was stored at room temperature for 16 weeks [the secant modulus at 2% ($E_{2\%}$) increased from 8.3 to 36.2 MPa and ultimate tensile strength (σ_u) from 6.4 to 16.3 MPa].

Herein, in order to assess the suitability of a mcl-PHA as an elastomeric biomaterial, the effects of a thermoplastic conformation process on the physical and mechanical properties of P(3HO-co-3HH) is evaluated in order to elucidate the relationship between molecular structure and mechanical properties in this semicrystalline thermoplastic elastomer. Several works in the literature have already investigated the effect of thermal history and associated outcomes (e.g., crystallinity, lamellar thickness, etc.) on the mechanical properties of traditional thermoplastic engineering polymers (e.g., polypropylene [24, 25], polyethylene [26], polyethylene terephthalate [27]) and biodegradable thermoplastic polymers [28-30]. Regarding PHAs, the majority of published studies have been focused on polyhydroxybutyrate (PHB) and PHB copolymers with hydroxyvalerate [31-35]. It has been reported that these (co)polymers undergo a dramatic embrittlement upon storage at room temperature, which can be ascribed to the development of secondary crystallization [36, 37] and associated vitrification of the rigid amorphous fraction [38-41]. In order to overcome this problem, copolymerization of hydroxybutyrate with medium chain length comonomers (i.e., hydroxyhexanoate) has been explored [42, 43]. Here it has been observed that for those copolymers with a fraction of hydroxyhexanoate higher than 10 mol.%, secondary crystallization was hampered due to steric hindrance and, accordingly, ductile mechanical behaviour was preserved for a period up to 60 days. However, these aforementioned studies were performed at room temperature and with short chain length

PHAs (scl-PHAs). In the study presented herein, P(3HO-co-3HH) was isothermally crystallized from the melt at four different temperatures between the T_g and the T_m (37, 21, 3 and -21 ºC) and the resulting molecular structures were analysed by differential scanning calorimetry (DSC) and wide-angle X-ray diffractometry (WAXD). Subsequently, the mechanical properties of these samples were analysed by tensile-tests and dynamic mechanical analysis (DMA). Finall the ability of these co-polymers to support cell viability was assessed *in vitro* through exposing L929 fibroblast cells to extraction media from mcl-PHA.

2. Materials and Methods

2.1. Materials

The P(3HO-co-3HH) employed in this work was kindly supplied by Neol Biosolutions (Spain) and synthesized as previously described [23]. Briefly, P(3HO-co-3HH) was produced by *P. putida*, a Gram-negative, saprotrophic bacterium, from octanoic acid and glycerol in a fed batch fermentation. The dried biomass was extracted with an organic solvent to obtain the raw polymer. In order to purify the raw material, it was mixed with a non-solvent which induced precipitation of the polymer. As determined by gel permeation chromatography (GPC), the synthesized P(3HO-co-3HH) showed a weight-averaged molecular weight (M_w) of 125 x 10^3 g mol^{-1} with a polydispersity index of 1.68. ^{13}C NMR results revealed that the synthesized P(3HO-co-3HH) was a copolymer with 94.3 and 5.7% of 3-hydroxyoctanoate and 3-hydroxyhexanoate, respectively.

2.2. Methods

2.2.1. Sample Preparation

Sheets of ~1 mm thickness were prepared by compression moulding in a Collin´s P200E hydraulic press at 140 ºC and 240 bar. Subsequently, the samples were

crystallized from the melt at four different temperatures: 37 ºC (oven), 21 ºC (room temperature), 3 ºC (fridge) and -21 ºC (freezer) and incubated at that temperature for 2 or 4 weeks until subsequent characterization. Samples were immediately transferred from the hydraulic press to the selected temperature to avoid crystallization during the transfer.

2.2.2. Differential Scanning Calorimetry (DSC)

Thermal transitions of P(3HO-co-3HH) were studied on a DSC 2920 (TA Instruments), which was equipped with a refrigerated cooling system (RSC 90). The calibration of enthalpy (cell) constant was performed with indium. The calculated heat of fusion of this standard was compared to the theoretical value and the cell constant was calculated from the ratio between these two values. Temperature calibration was also performed with indium. The extrapolated onset of the recorded melting point of this standard was compared to the known melting point and the difference was calculated for temperature calibration.

For the experiments, samples of 5-10 mg were first heated from -90 to 140 ºC at 20 ºC min^{-1} to erase the thermal history of the bulk polymer. Afterwards, the sample was cooled down from the melt and maintained isothermally at the selected temperature (37, 21, 3 or -21ºC) for 24 h. Finally, the sample was quenched within the DSC and a second scan was performed from -90 to 140 ºC to determine the T_g, T_m and heat of fusion (ΔH_f) of the polymer.

A heating DSC scan of the samples stored at the selected temperatures (37, 21, 3 or -21ºC) for 2 and 4 weeks was also performed from -90 to 140 ºC at 20 ºC min^{-1}.

2.2.3. Wide-angle X-ray Diffractometry

XRD data were collected on a Bruker D8 Advance diffractometer operating at 30 kV and 20 mA, equipped with a Cu tube (λ= 1.5418 Å), a Vantec-1 PSD detector and an Anton Parr MRI low-temperature chamber. The powder patterns were recorded in 2θ steps of 0.033° in the 10º<2θ<40° range, counting for 1s per step. Data sets were recorded isothermally at 37, 21, 3 and -21 ºC during 24 h after a 10 °C/min cooling ramp.

The X-ray diffraction signals were evaluated using the Diffrac Plus Evaluation EVA software. After extracting the amorphous halo in the 16-18º 2θ range, the raw area and half-width parameter of the diffraction maxima of the crystal part were calculated.

The deconvolution of the principal diffraction maxima was used to calculate the broadening of the diffraction lines for the 21.5º 2θ overlapped peak positions using the peak-fit option of WinPLOTR. The average size of the crystalline domains (coherently diffracting domains) of the sample was extracted from the broadening of the signal using the Scherrer equation [44]:

$$\beta_{hkl} = k \cdot \lambda / L_{hkl} \cdot \cos\theta$$

where β_{hkl} is the broadening of the diffraction line measured at half the line maximum intensity (FWHM) taking into account instrumental contribution (β_{Inst}=0.1°), λ is the X-ray wavelength, L_{hkl} is the crystal size and θ is the diffraction angle. k is the Scherrer shape factor (k=0.9 was assumed).

2.2.4. Tensile test

After an incubation at the selected temperatures (37, 21, 3 or -21ºC) for 2 and 4 weeks, tensile tests of dumbbell-shaped samples were performed with an Instron 5565 testing

machine at a crosshead displacement rate of 10 mm min^{-1}. This test was performed at 21±2 ºC and 50±5% relative humidity following ISO 527-2 (ISO 527-2/5A/1).

2.2.5. Dynamic Mechanical Analysis (DMA)

Dynamic mechanical measurements of samples stored at the selected temperatures (37, 21, 3 or -21ºC) for 4 weeks were carried out using a DMA/SDTA861e (Mettler Toledo) in tensile mode. The samples (length: 5.5. mm, width: 4 mm, thickness: 1 mm) were heated from -60 to 5 ºC at 3 ºC min^{-1}. The displacement and force amplitude were adjusted to 25 µm and 1.5 N, respectively, with a frequency of 1 Hz.

2.2.6. Evaluation of the Cytotoxicity

Mouse fibroblast (L929) were purchased from the American Type Culture Collection (ATC, USA). L929 cells were cultured in Minimum Essential Medium (MEM) (Gibco, USA) supplemented with 2 mM L-glutamine (Gibco, USA), 1% non-essential amino acids (NEAA) (Gibco, USA), 1.5 g L^{-1} of sodium bicarbonate (Gibco, USA), 1 mM sodium pyruvate (Gibco, USA), 100 UI ml^{-1} penicillin (Biochrom AG, Germany), 100 µg ml^{-1} streptomycin (Biochrom, Germany) and 10% fetal bovine serum (FBS) (Biochrom AG, Germany). Cultures were maintained in a humidified atmosphere (5% CO_2, 95% relative humidity) at 37 ºC. The cell medium was replacd every 2 days.

For *in vitro* cytotoxicity tests, P(3HO-co-3HH) samples were first sterilized by ethylene oxide. Subsequently, following ISO 10993-12 [45], extract fluid was prepared by submerging the samples in culture media for 24 h at 37 ºC in a humidified atmosphere containing 5% CO_2. To provide the basis for a comparison of the effect of the test material, culture medium, a negative control (i.e, its leachables have been demonstrated to be no cytotoxic: high-density polyethylene, USP Rockville, USA) and a positive control (i.e., its leachables have been demonstrated to be highly cytotoxic: polyvinyl

chloride, Portex Ltd, UK) were also employed. To assess the cytotoxicity of P(3HO-co-3HH), ISO/EN 10933 part 5 guidelines were followed: medium extraction with a 24 h extraction period and MTT assay to establish the possible toxic effect of leachables released from polymers during extraction [46]. L929 cells were plated in 96-well plates at a density of 4000 cells/well. After 24 h, the cell medium was replaced by extract fluid and cells were incubated for an additional 24, 48 and 72 h. Toxicity was then determined by a colorimetric assay (Cell Proliferation Kit MTT, Roche, Switzerland). In this assay, metabolically active cells are able to reduce the MTT to formazan pigment, which is dissolved in 100 µL dimethyl sulphoxide (DMSO) after removal of the culture medium. The metabolic activity of cells was finally determined by measuring the absorbance at 540 nm on a plate reader.

3. Results and Discussion

3.1. Short-term Crystallization

In order to study the effect of crystallization temperature on the supramolecular organization and on the crystallization kinetics of P(3HO-co-3HH), samples were first crystallized from the melt at the temperatures of interest (37, 21, 3 or -21ºC) for 24 h within the DSC. Afterwards, a heating scan from -90 to 140 ºC was performed to elucidate the thermal transitions of the polymer (Figure 1). The crystallization temperature did not have any significant effect on the T_g of P(3HO-co-3HH), which was ~-35 ºC in all the cases. However, the T_m gradually increased with the crystallization temperature. For example, T_m was 39.5 ºC when the crystallization temperature was -21 ºC, whereas it took a value of 62.5 ºC when the crystallization temperature was 37 ºC. Moreover, the melting peak became more defined at higher temperatures. It has been widely reported that when the crystallization occurs closer to the melting point, polymer chains reorganize themselves into more ordered crystalline domains with narrower

crystal distribution [28, 30]. This results in an increased lamellar thickness that shows increased melting points and narrower melting peaks [47]. A trend in ΔH_f with crystallization temperature was not clearly observed for P(3HO-co-3HH), which appeared to be maximum when the crystallization temperature was 3 ºC (ΔH_f = 26.2 J g^{-1}).

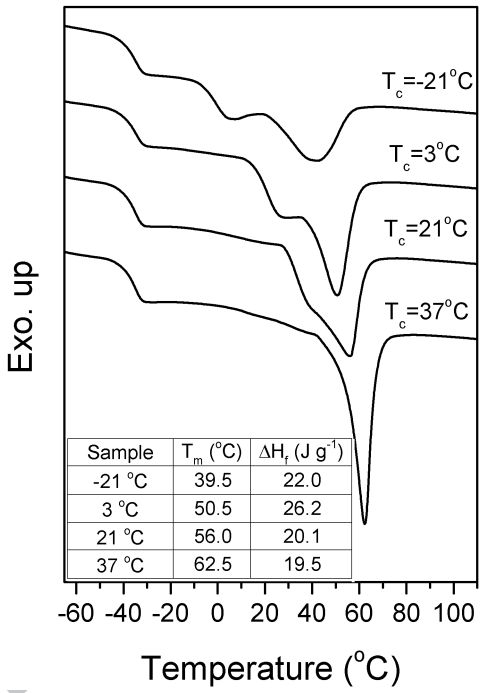

Sample	T_m (°C)	ΔH_f (J g^{-1})
-21 °C	39.5	22.0
3 °C	50.5	26.2
21 °C	56.0	20.1
37 °C	62.5	19.5

Figure 1. DSC thermograms of P(3HO-co-3HH) crystallized at the temperatures of interest for 24 h. T_c indicates the temperature at which the isothermal crystallization was performed.

Figure 2a and 2c shows the evolution with time of the integrated area of the WAXD diffractograms after subtracting the amorphous halo for P(3HO-co-3HH) crystallized from the melt at the temperatures of interest (37, 21, 3 or -21ºC). As it can be concluded from this graph, samples crystallized at 3 and 21ºC underwent the fastest rate of crystallization, being that of samples crystallized at 3ºC slightly faster than at 21ºC. The estimated coherent diffraction domain in these two cases was approximately 15 nm. In contrast, samples crystallized at 37 and -21ºC needed more time to develop crystalline domains. In this sense, first peaks in the diffractograms were observed after ~500 and

~350 min respectively for the samples isothermally crystallized at 37 and -21 ºC. The samples crystallized at 37 ºC displayed higher values in the estimated coherent diffraction domain (20 nm for the sample crystallized at 37 ºC *vs.* 15 nm for the rest of the samples). It has to be considered that the coherent diffraction domains estimated herein are an approximation and should not be considered as absolute values. In fact, the increasing melting temperatures observed in Figure 1 for samples crystallized at increasing temperatures suggest larger crystal sizes, that were not observed by WAXD analysis.

The crystallization kinetics of P(3HO-co-3HH) observed herein via WAXD measurements are in agreement with those previously determined by means of DSC for P(3HO-co-3HH) [23] and a similar copolymer composed of 10% hydroxyhexanoate, 86% hydroxyoctanoate and 4% hydroxydecanoate [48]. According to these studies, the most rapid crystallization of this copolymer occurred in the temperature range of 0-5ºC. At the end of the isothermal treatment (24 h), the values of the integrated area were similar for all the samples, indicating a similar volume of crystalline phase, which is in accordance with those results depicted in Figure 1 (i.e., similar ΔH_f values for all the samples after 24 h).

In all the cases after the deconvolution of the diffraction signal the relation between the amorphous and the crystalline part were similar. Nevertheless, the progressive decrease in signal intensity of some reflections (18º 2θ) indicates a loss of symmetry, probably a long-range order one (Figure 2b).

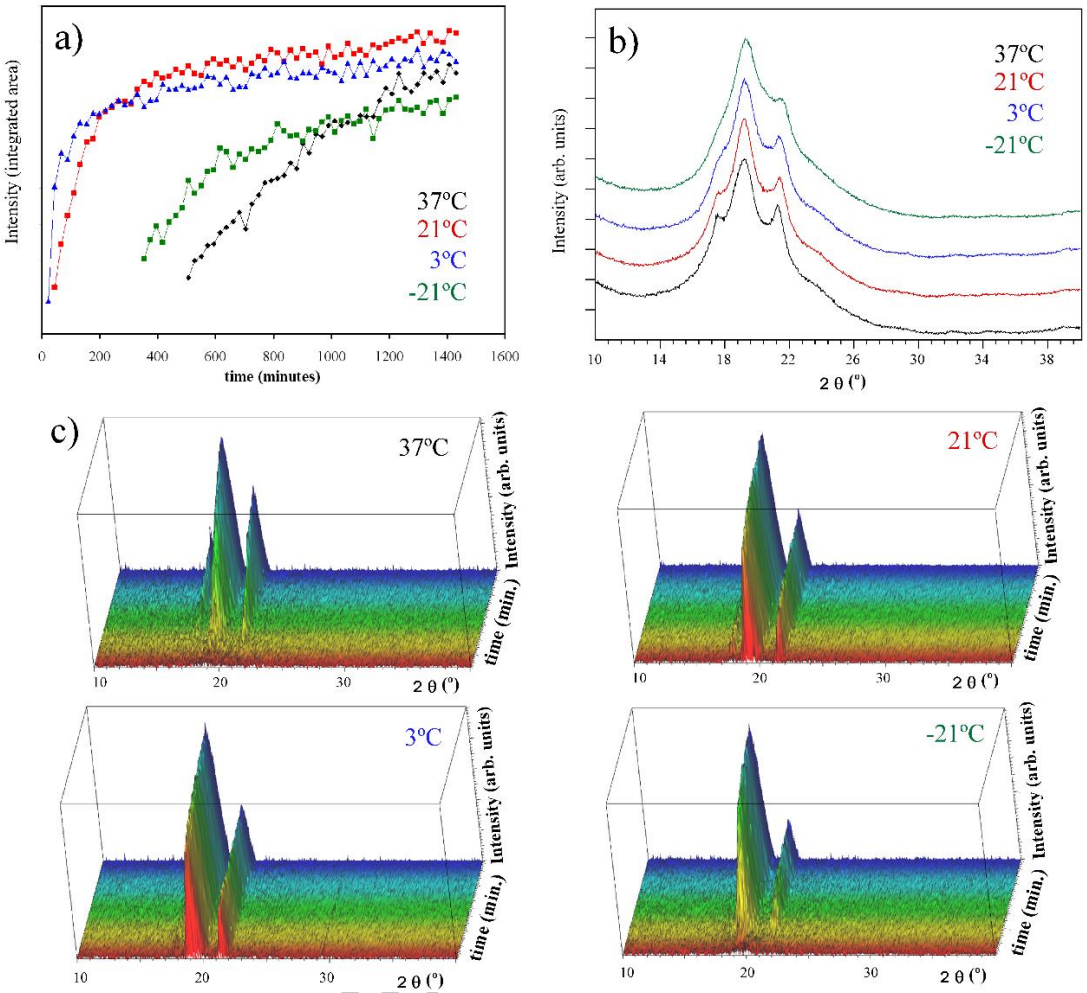

Figure 2. Evolution of the integrated area of the crystal part of the diffractograms after subtracting the amorphous halo (a). WAXD complete diffractograms of P(3HO-co-3HH) crystallized after 24 h at (37, 21, 3 or -21ºC) (b). Evolution of the crystal diffraction signals at the interest temperatures (37, 21, 3 or -21ºC) during 24 h isotherm (c).

3.2. Long-term Crystallization and its Effect on the Mechanical Properties

Figure 3 shows DSC thermograms of P(3HO-co-3HH) samples isothermally crystallized at the temperatures of interest (37, 21, 3 or -21ºC) for 2 and 4 weeks and their corresponding stress-strain curves. As previously observed in the short-term crystallization experiment (Figure 1), the crystallization temperature had a negligible effect on the T_g of P(3HO-co-3HH). Additionally, no differences associated to this transition in terms of specific heat capacity (Δc_p) and the temperature at which the transition occurs were observed with crystallization time. In similar studies dealing with

the evolution of glass transition of PHB with storage time, a decrease in Δc_p and an increase of T_g due to the presence of adjacent crystallites that constrain the amorphous domains was observed with crystallization time [36, 38, 41]. In view of this considerations, it can be assumed that the resulting mechanical properties reported by us are mainly determined by the different crystal "perfections" rather than to a process associated with the amorphous phase (i.e., evolution of the rigid amorphous fraction).

The selected crystallization temperature clearly determines how polymer chains are reorganized into crystalline domains. Accordingly, higher crystallization temperatures resulted in better defined melting peaks and higher T_m values, which suggest more ordered crystalline domains with narrower crystal distribution. For example, the calculated T_m values for samples crystallized at 37, 21, 3 and -21 ºC for 2 weeks were respectively, 65, 60, 56 and 51 ºC. In general, ΔH_f values slightly increased between week 2 and 4 but the differences were almost negligible, indicating that after 2 weeks the polymer may have reached a quasi-equilibrium state. These values were very similar for those samples crystallized at 37, 21 and 3 ºC but was clearly lower for the sample crystallized at -21 ºC. In this sense, ΔH_f was 21.1 J g^{-1} for the sample crystallized at -21 ºC after 4 weeks, whereas it took values in the range of 24.8-25.7 J g^{-1} for the rest of the samples.

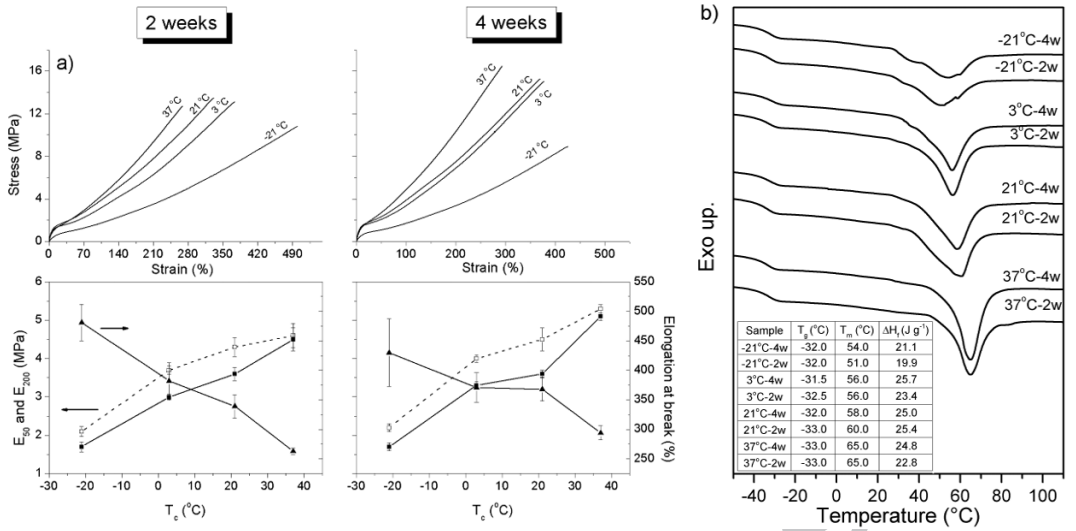

Sample	T_g (°C)	T_m (°C)	ΔH_f (J g^{-1})
-21°C-4w	-32.0	54.0	21.1
-21°C-2w	-32.0	51.0	19.9
3°C-4w	-31.5	56.0	25.7
3°C-2w	-32.5	56.0	23.4
21°C-4w	-32.0	58.0	25.0
21°C-2w	-33.0	60.0	25.4
37°C-4w	-33.0	65.0	24.8
37°C-2w	-33.0	65.0	22.8

Figure 3. Tensile-test curves of P(3HO-co-3HH) crystallized at the temperatures of interest (37, 21, 3 and -21ºC) for 2 and 4 weeks (a) and the corresponding DSC thermograms (b).

As observed in Figure 3a and Table 1, the mechanical properties of the samples were clearly affected by the parameters mentioned above. In all the cases, the secant modulus ($E_{2\%}$) slightly increased between week 2 and week 4, which can be attributed to a slightly higher crystallinity fraction (i.e., higher ΔH_f values) and concurrent vitrification of the rigid amorphous fraction [41]. For samples crystallized at 37, 21 and 3ºC, $E_{2\%}$ did not follow a particular trend and was in the range of 16.8-18.2 MPa and 19.5-22.6 MPa after 2 and 4 weeks respectively. In contrast, samples crystallized at -21ºC displayed a much lower $E_{2\%}$ (6.6 and 7.0 MPa at week 2 and 4, respectively). It is well accepted that Young´s modulus (or, in this case, the secant modulus calculated at 2%) increases with crystallinity [25]. Herein, this clear differences on the $E_{2\%}$ between the sample crystallized at -21 ºC and the rest of the samples are associated to the different degrees of crystallinity observed in DSC (Figure 3b).

Table 1. Mechanical properties of PHA samples stored at -21, 3, 21 and 37 ºC during 2 or 4 weeks.

Sample	*$E_{2\%}$ (MPa)*	*$E_{50\%}$ (MPa)*	*$E_{100\%}$ (MPa)*	*$E_{200\%}$ (MPa)*	*σ_y (10%) (MPa)*	*σ_u (MPa)*	*ε_u (%)*	*Strain recovery (%)*
-21ºC-2w	6.6 ± 1.2	2.1 ± 0.1	1.7 ± 0.1	1.7 ± 0.1	0.8 ± 0.1	10.3 ± 0.9	481 ± 31	37 ±1
-21ºC-4w	7.0 ± 0.5	2.2 ± 0.1	1.7 ± 0.1	1.7 ± 0.1	0.8 ± 0.1	9.2 ± 1.9	430 ± 57	38 ± 1
3ºC-2w	17.2 ± 1.1	3.7 ± 0.1	3.0 ± 0.1	3.0 ± 0.1	1.3 ± 0.1	13.7 ± 1.5	382 ± 31	33 ± 1
3ºC-4w	22.6 ± 1.6	4.0 ± 0.1	3.3 ± 0.1	3.3 ± 0.1	1.5 ± 0.1	14.5 ± 1.4	371 ± 25	31 ± 1
21ºC-2w	18.2 ± 2	4.3 ± 0.3	3.6 ± 0.2	3.6 ± 0.2	1.5 ± 0.1	13.4 ± 1.4	339 ± 20	31 ± 2
21ºC-4w	20.8 ± 2.8	4.5 ± 0.3	3.8 ± 0.1	3.6 ± 0.1	1.5 ± 0.1	14.9 ± 0.7	368 ± 20	35 ± 1
37ºC-2w	16.8 ± 1.3	4.6 ± 0.3	4.2 ± 0.3	4.5 ± 0.3	1.4 ± 0.1	12.6 ± 0.7	263 ± 5	26 ± 1
37ºC-4w	19.5 ± 0.4	5.3 ± 0.1	4.7 ± 0.1	5.1 ± 0.1	1.7 ± 0.3	16.2 ± 0.7	294 ±12	27 ± 1

Secant moduli calculated at 50, 100 and 200% ($E_{50\%}$, $E_{100\%}$ and $E_{200\%}$) slightly increased in all the cases between week 2 and week 4. Moreover, a clear trend in these values with the crystallization temperature was observed, showing a positive correlation (i.e., higher crystallization temperatures result in higher $E_{50\%}$, $E_{100\%}$ and $E_{200\%}$ values). As an illustration, $E_{200\%}$ after 4 weeks was 1.7, 3.3, 3.6 and 5.1 MPa for the samples crystallized at -21, 3, 21 and 37 ºC, respectively. Similar trend was also observed for the offset yield strength (σ_y) calculated at 10% of strain using the secant modulus at 2% as elastic modulus. For example, σ_y was 0.8 MPa for the sample crystallized at -21 ºC after 4 weeks, whereas it took a value of 1.7 MPa for the sample crystallized at 37 ºC during the same period of time. It has been observed in several studies that yield behaviour of polymers is proportional to lamellar/crystal thickness [27], being this proportionality true both above and below the T_g [49]. Accordingly, polymeric samples displaying similar degrees of crystallinity can show completely different mechanical behaviour depending on the lamellar/crystal thickness [26]. In this particular study, as previously demonstrated by DSC and WAXD, those samples crystallized at higher temperatures showed higher melting temperatures and better defined diffraction peaks. This suggests more ordered crystalline domains that play a role in the resulting mechanical properties of the samples.

Finally elongation at break (ε_u) and strain recovery after break of the samples generally decreased when the samples were crystallized at higher temperatures. On the one hand, ε_u was 294, 368, 371 and 430% for samples crystallized at 37, 21, 3 and -21 ºC for 4 weeks, respectively. It has to be highlighted that, in contrast to other reported PHA materials [35, 39], the mcl-PHA explored in this study did not undergo a dramatic embrittlement with storage time and maintained a high elongation at break in all cases. As previously reported [43], mcl-PHAs are able to preserve their ductile behaviour with time more efficiently than scl-PHAs due to their intrinsically lower crystallinity and thicker amorphous region. Strain recovery was 38% for samples crystallized at -21 ºC for 4 weeks, whereas it was 27% for the sample crystallized at 37 ºC for the same period of time.

The effect of crystallization temperature was also analysed by means of dynamic mechanical analysis. The temperature dependent curves of storage modulus (E´) and tanδ for P(3HO-co-3HH) after being crystallized from the melt at the temperatures of interest (37, 21, 3 or -21ºC) for 4 weeks are presented in Figure 4. The values of tanδ for the samples crystallized at 37, 21, 3 and -21 ºC were respectively, 0.43, 0.44, 0.40 and 0.49. The value of tanδ is positively correlated with the amorphous fraction in a polymeric sample [50] (i.e., it tooks higher values for polymeric samples with higher amorphous fraction/lower degrees of crystallinity). For this reason, the sample crystallized at -21 ºC showed slightly higher values of tanδ, which is in accordance with the ΔH_f values presented in Figure 3. Little differences were observed in the tanδ values for the rest of the samples (i.e., those crystallized at 37, 21 and 3 ºC), being slightly lower for the sample crystallized at 3 ºC, which displays the highest ΔH_f in Figure 3. The storage modulus (E´), which is usually associated to the Young´s modulus, above the glass transition followed the same trend as that observed for $E_{2\%}$ in the tensile tests.

In this sense, samples crystallized at 3 ºC showed the highest E´, followed by samples crystallized at 21 and 37 ºC and finally, by the sample crystallized at -21 ºC. In summary, the conclusions obtained from dynamic mechanical analysis are in accordance with the previous results presented herein and depend on the degree of crystallinity of the sample rather than on the lamellar/crystal thickness.

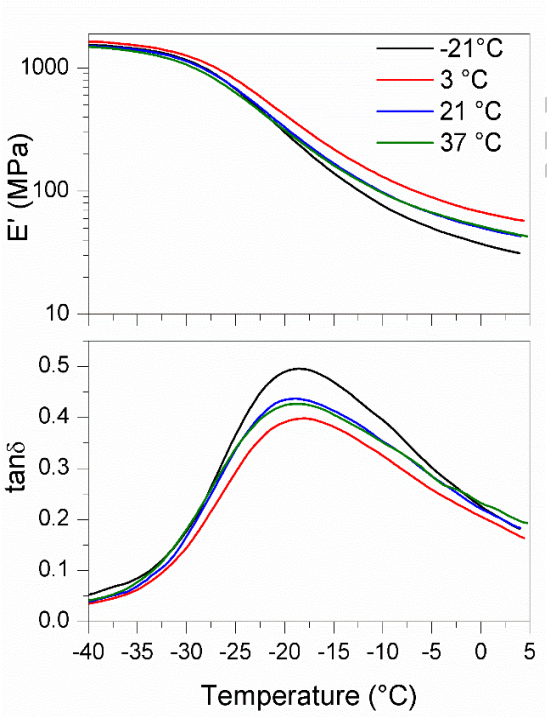

Figure 4. Storage modulus (E´) and tanδ curves of the P(3HO-co-3HH) crystallized at the temperatures of interest (37, 21, 3 and -20 ºC) for 4 weeks.

3.3. Evaluation of the Cytotoxicity of P(3HO-co-3HH)

Figure 5 shows the metabolic activity of L929 cells cultured with the extracts of P(3HO-co-3HH) determined via the MTT assay. This colorimetric assay is based on the cleavage of the tetrazolium salt (i.e., MTT) to water-insoluble formazan salt by metabolically active cells. Therefore, the amount of formazan produced, which can be measured at 540 nm after being solubilized in DMSO, directly correlates with the number of metabolically active cells in culture. The cellular response to the negative and positive control materials was as expected in all tests, confirming the validity of the

assay. L929 cells displayed similar metabolic profiles to those obtained from cells grown in standard culture medium or under negative control conditions. This demonstrates that cells grown in P(3HO-co-3HH) extract were able to metabolize MTT, indirectly inferring persistance of viability and normal proliferation activity. In view of these results, it can be considered that leachables released from P(3HO-co-3HH) are non-cytotoxic. The mcl-PHA employed in this work also demonstrated its ability to promote neuronal cell growth [18]. Taken together, the results presented herein and the ones recently published by our group, suggest that the P(3HO-co-3HH) may be considered for biomedical applications demanding bioresorbable polymers with soft mechanical properties.

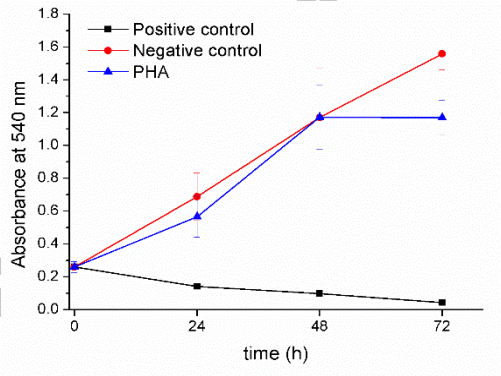

Figure 5. Metabolic activity of L929 cells grown in P(3HO-co-3HH), positive (polyvinyl chloride) and negative (high-density polyethylene) control extract media.

4. Conclusions

PHAs are gaining increasing interest in the biomedical field due to their biodegradability, biocompatibility and processability. The most widely reported polyhydroxybutyrate and its copolymers with hydroxyvalerate have been reported to undergo a dramatic embrittlement when stored at room temperature that can limit their potential use in the biomedical field. For that reason, mcl-PHAs, such as the P(3HO-co-3HH) presented herein, may represent a promising alternative to the aforementioned (co)polymers.

In the present work the effect of isothermal crystallization on the mechanical properties of an elastomeric thermoplastic polymer was studied. P(3HO-co-3HH) was isothermally crystallized from the melt at four temperatures between its T_g and T_m (37, 21, 3 and -21 ºC) for two and four weeks. Samples crystallized at -21 ºC showed a lower degree of crystallinity and therefore, displayed lower secant modulus relative to samples crystallized at 37, 21 and 3 ºC. Interestingly, samples crystallized at 37, 21 and 3 ºC showed very similar degrees of crystallinity but displayed different mechanical properties which can be associated to different crystalline structures. As determined by DSC and WAXD, higher crystallization temperatures resulted in more ordered crystalline structure and narrower crystal distribution. Accordingly, secant modulus calculated at 50, 100 and 200% of strain and yield strength increased with the crystallization temperature, whereas elongation at break decreased. Interestingly, samples did not undergo a dramatic embrittlement with storage time and keep high elongations at break in all cases. The polymer employed in this work did not elicit any cytotoxic response on L929 cells and may find potential use in biomedical applications demanding "soft" and elastomeric biodegradable polymers with tuneable mechanical properties.

Acknowledgments

The authors are thankful for funds from the Basque Government, Department of Education, Universities and Research (GIC12/161-IT-632-13) and the Spanish Ministry of Innovation and Competitiveness MINECO (MAT2013-45559-P).

References

[1] Lee SY. Bacterial polyhydroxyalkanoates. Biotechnology and Bioengineering. 1996;49:1-14.
[2] Lee SY. Plastic bacteria? Progress and prospects for polyhydroxyalkanoate production in bacteria. Trends in Biotechnology. 1996;14:431-8.
[3] Muhammadi, Shabina, Afzal M, Hameed S. Bacterial polyhydroxyalkanoates-eco-friendly next generation plastic: Production, biocompatibility, biodegradation, physical properties and applications. Green Chemistry Letters and Reviews. 2015;8:56-77.
[4] Sudesh K, Abe H, Doi Y. Synthesis, structure and properties of polyhydroxyalkanoates: biological polyesters. Progress in Polymer Science. 2000;25:1503-55.
[5] Fernández J, Meaurio E, Chaos A, Etxeberria A, Alonso-Varona A, Sarasua JR. Synthesis and characterization of poly (l-lactide/ε-caprolactone) statistical copolymers with well resolved chain microstructures. Polymer. 2013;54:2621-31.
[6] Tanzi MC, Verderio P, Lampugnani MG, Resnati M, Dejana E, Sturani E. Cytotoxicity of some catalysts commonly used in the synthesis of copolymers for biomedical use. Journal of Materials Science: Materials in Medicine. 1994;5:393-6.
[7] Stjerndahl A, Finne-Wistrand A, Albertsson AC, Bäckesjö CM, Lindgren U. Minimization of residual tin in the controlled Sn(II)octoate-catalyzed polymerization of ε-caprolactone. Journal of Biomedical Materials Research Part A. 2008;87A:1086-91.
[8] Fernandez J, Larranaga A, Etxeberria A, Sarasua J-R. Ethylene brassylate-co-δ-hexalactone biobased polymers for application in the medical field: synthesis, characterization and cell culture studies. RSC Advances. 2016;6:22121-36.
[9] Kricheldorf HR. Syntheses of Biodegradable and biocompatible polymers by means of bismuth catalysts. Chemical Reviews. 2009;109:5579-94.
[10] Saito Y, Nakamura S, Hiramitsu M, Doi Y. Microbial synthesis and properties of poly(3-hydroxybutyrate-co-4-hydroxybutyrate). Polymer International. 1996;39:169-74.
[11] Di Lorenzo ML, Raimo M, Cascone E, Martuscelli E. Poly(3-hydroxybutyrate)-based copolymers and blends: influence of a second component on crystallization and thermal behavior. Journal of Macromolecular Science, Part B. 2001;40:639-67.
[12] Barrett JSF, Abdala AA, Srienc F. Poly(hydroxyalkanoate) elastomers and their graphene nanocomposites. Macromolecules. 2014;47:3926-41.
[13] Misra SK, Valappil SP, Roy I, Boccaccini AR. Polyhydroxyalkanoate (PHA)/inorganic phase composites for tissue engineering applications. Biomacromolecules. 2006;7:2249-58.
[14] Zinn M, Witholt B, Egli T. Occurrence, synthesis and medical application of bacterial polyhydroxyalkanoate. Advanced Drug Delivery Reviews. 2001;53:5-21.
[15] Pontailler M, Illangakoon E, Williams GR, Marijon C, Bellamy V, Balvay D, et al. Polymer-based reconstruction of the inferior vena cava in rat: stem cells or RGD peptide? Tissue Eng Pt A. 2015;21:1552-64.
[16] Wu S, Liu YL, Cui B, Qu XH, Chen GQ. Study on decellularized porcine aortic valve/poly (3-hydroxybutyrate-co-3-hydroxyhexanoate) hybrid heart valve in sheep model. Artif Organs. 2007;31:689-97.
[17] Masaeli E, Wieringa PA, Morshed M, Nasr-Esfahani MH, Sadri S, van Blitterswijk CA, et al. Peptide functionalized polyhydroxyalkanoate nanofibrous scaffolds enhance Schwann cells activity. Nanomed-Nanotechnol. 2014;10:1559-69.
[18] Vallejo-Giraldo CP, E.; Larrañaga, A.; Fernandez-Yague, M.A.; Britton, J.J.; Trotier, A.; Taddayon, G.; Kelly, A.; Scaini, D.; Sarasua, J.R.; Dowd, E.; Quinlan, E.; Pandit, A.; Biggs, M.J.P. Polyhydroxyalkanoate/carbon nanotube nanocomposites: flexible electrically conducting elastomers for neural applications. Nanomedicine-Future Medicine. 2016;11:2547-63.
[19] Wei X, Hu YJ, Xie WP, Li RL, Chen GQ. Influence of poly(3-hydroxybutyrate-co-4-hydroxybutyrate-co-3-hydroxyhexanoate) on growth and osteogenic differentiation of human bone marrow-derived mesenchymal stem cells. Journal of Biomedical Materials Research Part A. 2009;90A:894-905.
[20] Rathbone S, Furrer P, Lubben J, Zinn M, Cartmell S. Biocompatibility of polyhydroxyalkanoate as a potential material for ligament and tendon scaffold material. Journal of Biomedical Materials Research Part A. 2010;93A:1391-403.
[21] Barouti G, Jarnouen K, Cammas-Marion S, Loyer P, Guillaume SM. Polyhydroxyalkanoate-based amphiphilic diblock copolymers as original biocompatible nanovectors. Polym Chem-Uk. 2015;6:5414-29.

[22] Rai R, Keshavarz T, Roether JA, Boccaccini AR, Roy I. Medium chain length polyhydroxyalkanoates, promising new biomedical materials for the future. Materials Science and Engineering: R: Reports. 2011;72:29-47.
[23] Larrañaga A, Fernández J, Vega A, Etxeberria A, Ronchel C, Adrio JL, et al. Crystallization and its effect on the mechanical properties of a medium chain length polyhydroxyalkanoate. Journal of the Mechanical Behavior of Biomedical Materials. 2014;39:87-94.
[24] Kristiansen M, Tervoort T, Smith P, Goossens H. Mechanical properties of sorbitol-clarified isotactic polypropylene: influence of additive concentration on polymer structure and yield behavior. Macromolecules. 2005;38:10461-5.
[25] Caelers HJM, Govaert LE, Peters GWM. The prediction of mechanical performance of isotactic polypropylene on the basis of processing conditions. Polymer. 2016;83:116-28.
[26] Kazmierczak T, Galeski A, Argon AS. Plastic deformation of polyethylene crystals as a function of crystal thickness and compression rate. Polymer. 2005;46:8926-36.
[27] Schrauwen BAG, Janssen RPM, Govaert LE, Meijer HEH. Intrinsic deformation behavior of semicrystalline polymers. Macromolecules. 2004;37:6069-78.
[28] Tsuji H, Ikada Y. Properties and morphologies of poly(l-lactide): 1. Annealing condition effects on properties and morphologies of poly(l-lactide). Polymer. 1995;36:2709-16.
[29] Pluta M. Morphology and properties of polylactide modified by thermal treatment, filling with layered silicates and plasticization. Polymer. 2004;45:8239-51.
[30] Lizundia E, Petisco S, Sarasua J-R. Phase-structure and mechanical properties of isothermally melt- and cold-crystallized poly (L-lactide). Journal of the Mechanical Behavior of Biomedical Materials. 2013;17:242-51.
[31] Androsch R. Surface structure of folded-chain crystals of poly(R-3-hydroxybutyrate) of different chain length. Polymer. 2008;49:4673-9.
[32] Srubar Iii WV, Wright ZC, Tsui A, Michel AT, Billington SL, Frank CW. Characterizing the effects of ambient aging on the mechanical and physical properties of two commercially available bacterial thermoplastics. Polymer Degradation and Stability. 2012;97:1922-9.
[33] de Koning GJM, Lemstra PJ, Hill DJT, Carswell TG, O'Donnell JH. Ageing phenomena in bacterial poly[(R)-3-hydroxybutyrate]. Polymer. 1992;33:3295-7.
[34] Scandola M, Ceccorulli G, Pizzoli M. The physical aging of bacterial poly(D-β-hydroxybutyrate). Die Makromolekulare Chemie, Rapid Communications. 1989;10:47-50.
[35] Daly JH, Hayward D, Liggat JJ, Mackintosh AR. Ageing and rejuvenation of Biopol™, [poly (3-hydroxybutyrate-co-3-hydroxyvalerate)] copolymers: A dielectric study. Journal of Materials Science. 2004;39:925-31.
[36] Biddlestone F, Harris A, Hay JN, Hammond T. The physical ageing of amorphous poly(hydroxybutyrate). Polymer International. 1996;39:221-9.
[37] Hurrell BL, Cameron RE. A wide-angle X-ray scattering study of the ageing of poly(hydroxybutyrate). Journal of Materials Science. 1998;33:1709-13.
[38] Di Lorenzo ML, Gazzano M, Righetti MC. The role of the rigid amorphous fraction on cold crystallization of poly(3-hydroxybutyrate). Macromolecules. 2012;45:5684-91.
[39] de Koning GJM, Lemstra PJ. Crystallization phenomena in bacterial poly[(R)-3-hydroxybutyrate]: 2. Embrittlement and rejuvenation. Polymer. 1993;34:4089-94.
[40] Di Lorenzo ML, Righetti MC. Evolution of crystal and amorphous fractions of poly[(R)-3-hydroxybutyrate] upon storage. Journal of Thermal Analysis and Calorimetry. 2013;112:1439-46.
[41] Di Lorenzo ML, Righetti MC. Effect of thermal history on the evolution of crystal and amorphous fractions of poly[(R)-3-hydroxybutyrate] upon storage at ambient temperature. European Polymer Journal. 2013;49:510-7.
[42] Asrar J, Valentin HE, Berger PA, Tran M, Padgette ST, Garbow JR. Biosynthesis and properties of poly(3-hydroxybutyrate-co-3-hydroxyhexanoate) polymers. Biomacromolecules 2002; 3: 1006-12.
[43] Alata H, Aoyama T, Inoue Y. Effect of aging on the mechanical properties of poly(3-hydroxybutyrate-co-3-hydroxyhexanoate). Macromolecules. 2007;40:4546-51.
[44] Scherrer P. Bestimmung der inneren struktur und der größe von kolloidteilchen mittels röntgenstrahlen. Kolloidchemie Ein Lehrbuch. Berlin, Heidelberg: Springer Berlin Heidelberg; 1912. p. 387-409.
[45] ISO 10993–12: Biological evaluation of medical devices -- Part 12: sample preparation and reference materials, 2002.
[46] ISO 10993–5: Biological evaluation of medical devices -- Part 5: tests for in vitro cytotoxicity, 2009.
[47] Barham PJ, Keller A, Otun EL, Holmes PA. Crystallization and morphology of a bacterial thermoplastic: poly-3-hydroxybutyrate. Journal of Materials Science. 1984;19:2781-94.

[48] Gagnon KD, Lenz RW, Farris RJ, Fuller RC. Crystallization behavior and its influence on the mechanical properties of a thermoplastic elastomer produced by Pseudomonas oleovorans. Macromolecules. 1992;25:3723-8.
[49] Brooks NWJ, Mukhtar M. Temperature and stem length dependence of the yield stress of polyethylene. Polymer. 2000;41:1475-80.
[50] Ugartemendia JM, Larrañaga A, Amestoy H, Sarasua JR. Supramolecular evolution over an initial period of biodegradation of lactide and caprolactone based medical (co)polyesters. Polymer Degradation and Stability. 2014;108:87-96.

EFFECTS OF ISOTHERMAL CRYSTALLIZATION ON THE MECHANICAL PROPERTIES OF A ELASTOMERIC MEDIUM CHAIN LENGTH POLYHYDROXYALKANOATE

A. Larrañaga, F. Pompanon, N. Gruffat, T. Palomares, A. Alonso-Varona, A. Larrañaga Varga, M.A. Fernandez-Yague, M.J.P. Biggs, J.R. Sarasua

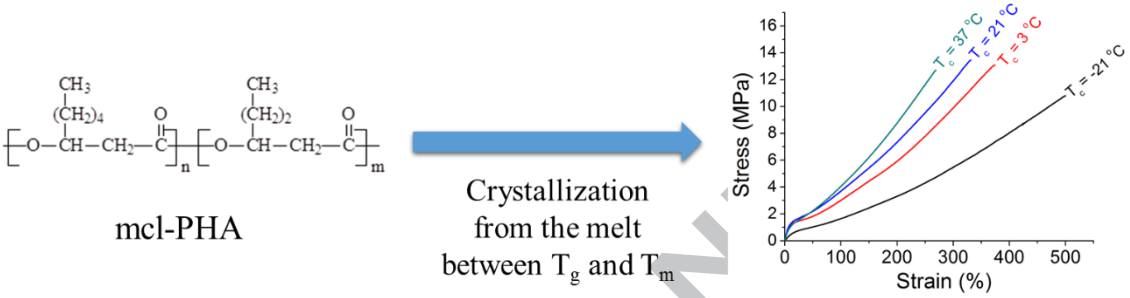

- Relationship between molecular structure and mechanical properties for a mcl-PHA is elucidated
- Higher crystallization temperature results in more ordered crystalline domains and narrower crystal distributions
- Higher crystallinity results in higher secant moduli calculated at 2% of deformation
- A positive correlation was found between crystallization temperature and secant moduli at 50, 100 and 200%